Electronic Supplementary Information

Characterization of neutral metal hydride-hydroxide hydrogen-bonded clusters $HMOH(H_2O)_2$ (M = Al and Ga)

Wenhui Yan,[1,2] Huijun Zheng,[1,2] Tiantong Wang,[1,2] Shuai Jiang,[1,2] Shangdong Li,[1,2] Jianxing Zhuang,[1,2] Hua Xie,[1,2] Gang Li,[1,2,*] and Ling Jiang[1,2,3,*]

1. State Key Laboratory of Molecular Reaction Dynamics and Dalian Coherent Light Source, Dalian Institute of Chemical Physics, Chinese Academy of Sciences, Dalian 116023, China.
2. University of Chinese Academy of Sciences, Beijing 100049, China.
3. Hefei National Laboratory, Hefei 230088, China.

*Corresponding authors.
E-mail addresses: gli@dicp.ac.cn (G. Li), ljiang@dicp.ac.cn (L. Jiang).

Experimental details

The experiments were carried out by using an IR-VUV apparatus, which was extensively described in the previous articles.[1-4] For cluster generation, a laser vaporization source was utilized to achieve supersonic expansion of a 0.2% H_2O/He mixture, resulting in the formation of neutral clusters $HMOH(H_2O)_2$ (M = Al and Ga). The aluminum and gallium metal targets (purity 99.9%) were ablated using a pulse energy of 1mJ from a Nd:YAG laser (Innolas, Spitlight 400) operating at 532 nm wavelength. The reaction gas was introduced via the Parker valve (series 009) with a pulse width of 220 μs. Subsequently, the molecular beam passed through a skimmer (Beam Dynamics, Model 50.8) with a diameter of 4mm, underwent ionization by ultraviolet light, and were detected by a reflection time-of-flight mass spectrometer. Charged clusters were deflected out of the molecular beam by the DC (+2950V) electric field of the extraction plates.

The tunable infrared light pulse was introduced approximately 60 ns before the VUV pulse in a cross-over manner. When the resonant vibrational transition was irradiated by the IR laser light and caused vibrational predissociation, a depletion of the selected neutral cluster mass signal was detected. The infrared spectra were recorded by the difference between the mass spectral signals without and with an infrared laser (IR laser OFF minus IR laser On). The IR spectra of size-specific neutral clusters (AlO_3H_6 and GaO_3H_6) were measured by a depletion spectrum of the ion signal intensity as a function of IR wavelength. The scanning of infrared wavelengths was performed in steps of 2 cm^{-1}, while averaging 600 laser shots at each wavelength to record a representative spectrum. In addition, the infrared energy dependence of the spectral signal was measured to ensure that the predissociation efficiency of the neutral cluster was linear with the infrared photon flux.

While the pulse valve, 532nm laser, and VUV light were operated at a frequency of 20 Hz, the tunable infrared light was operated at a frequency of 10 Hz. To produce VUV light at a wavelength of 193 nm with an energy per pulse of 14 mJ, an ArF excimer laser (Coherent, GAMLAS EX5A) was employed. Additionally, the infrared laser was

generated by a potassium titanyl phosphate/potassium titanyl arsenate optical parametric oscillator/amplifier system (OPO/OPA, Laser Vision) pumped by an injection-seeded Nd:YAG laser (Continuum, Surelite EX). The OPO/OPA system allowed for adjustment within the range of 700 to 7000 cm^{-1} with a line width set at approximately 1 cm^{-1}. The wavelength of the OPO laser output was calibrated by using a commercial wavelength meter (HighFinesse GmbH, WS6-200 VIS IR).

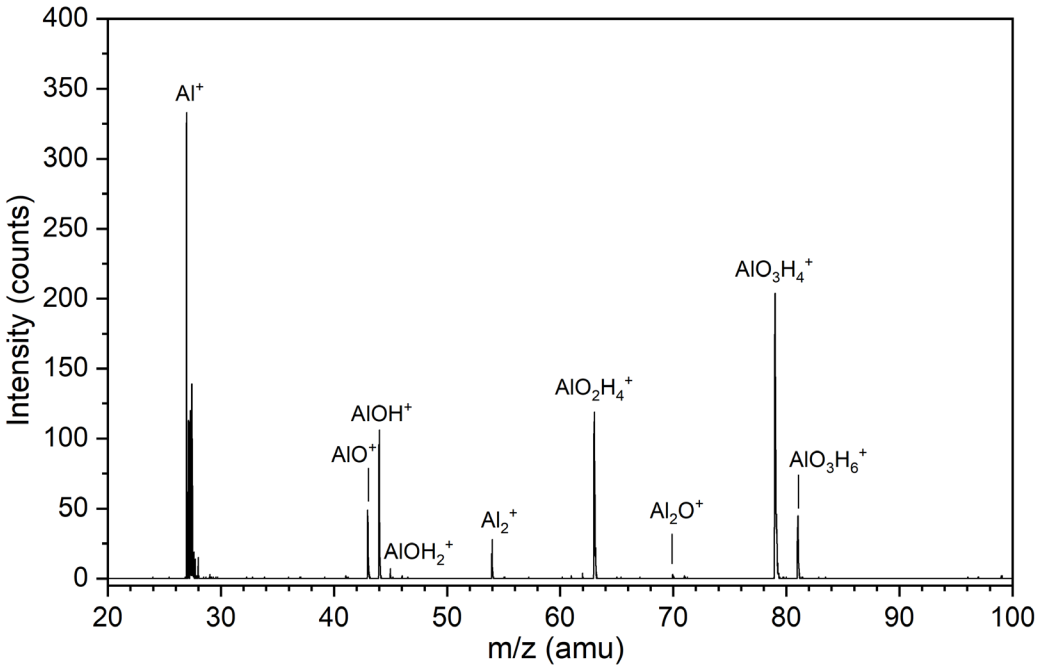

Figure S1. Time-of-flight mass spectrum of the cations produced from the VUV ionization of the Al + H_2O reaction.

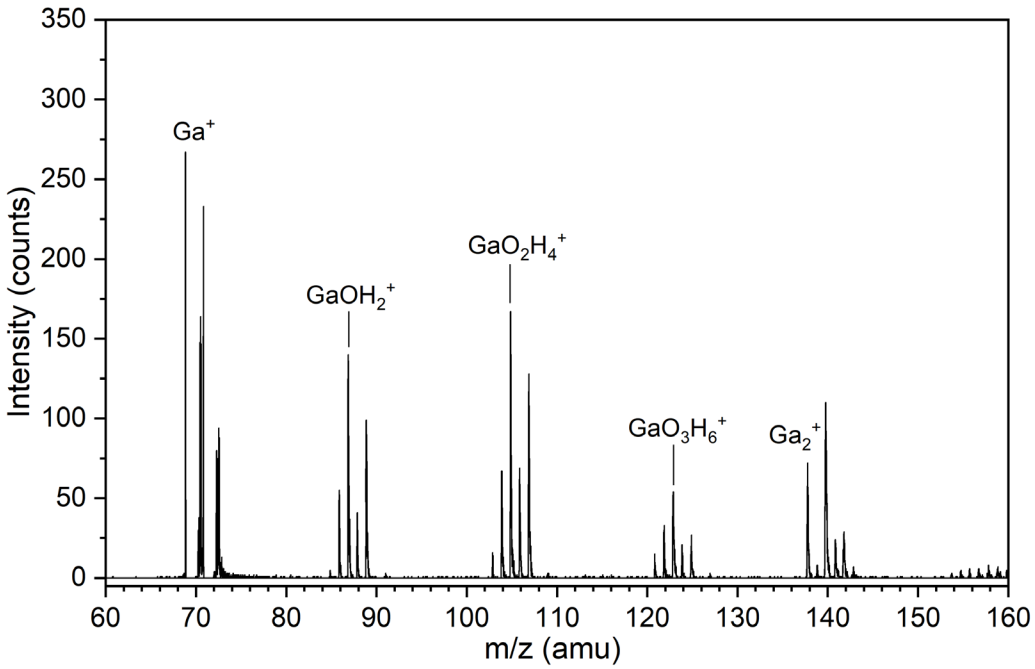

Figure S2. Time-of-flight mass spectrum of the cations produced from the VUV ionization of the Ga + H_2O reaction.

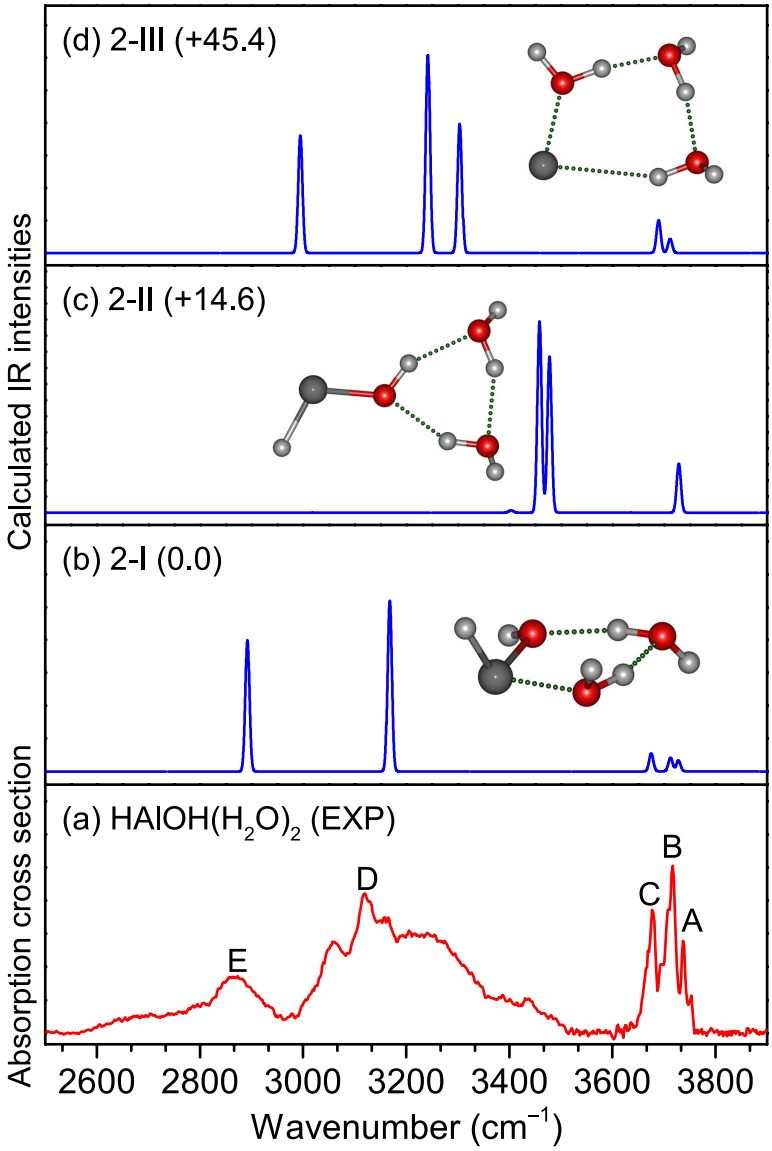

Figure S3. Comparison of experimental IR spectrum of neutral $HAlOH(H_2O)_2$ complex (a) and MP2/aug-cc-pVDZ calculated harmonic IR spectra of the three lowest-energy isomers (b-d). The structures (O, red; H, light gray; Al, gray) are embedded in the inset. The relative energies are given in kcal/mol.

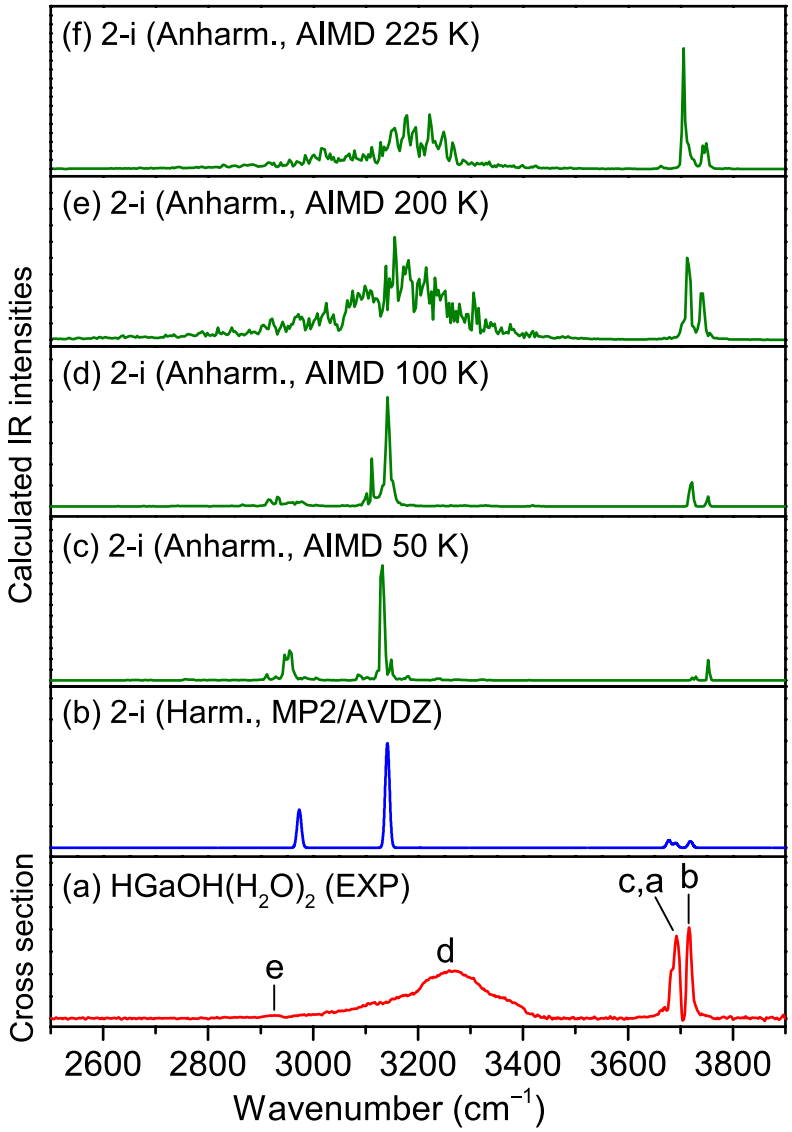

Figure S4. Comparison of experimental IR spectrum of neutral $HGaOH(H_2O)_2$ complex (a) and MP2/aug-cc-pVDZ calculated harmonic IR spectrum of isomer 2-i (b) and AIMD simulated spectra at 50 K, 100 K, 200 K, and 225 K (c-f) of isomer 2-i.

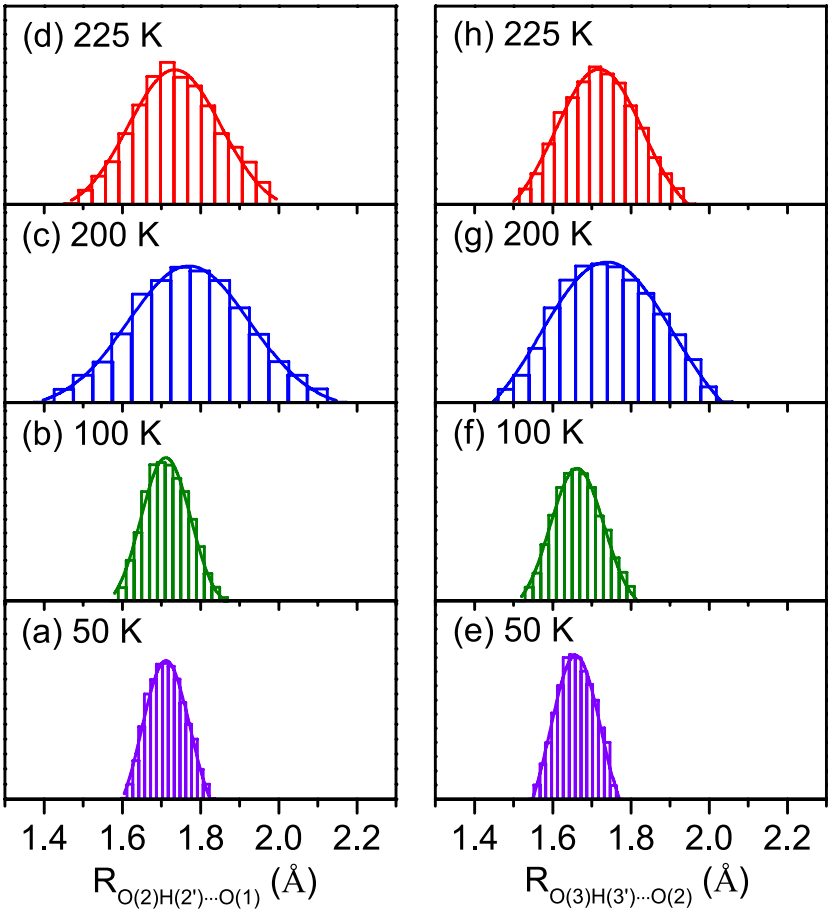

Figure S5. Normal distribution of O(2)H(2′)···O(1) and O(3)H(3′)···O(2) hydrogen-bond distances ($R_{O(2)H(2')\cdots O(1)}$ and $R_{O(3)H(3')\cdots O(2)}$) during AIMD simulations of isomer 2-i for $HGaOH(H_2O)_2$ at 50 K, 100 K, 200 K, and 225 K. The atom labelling is indicated in Figure 2.

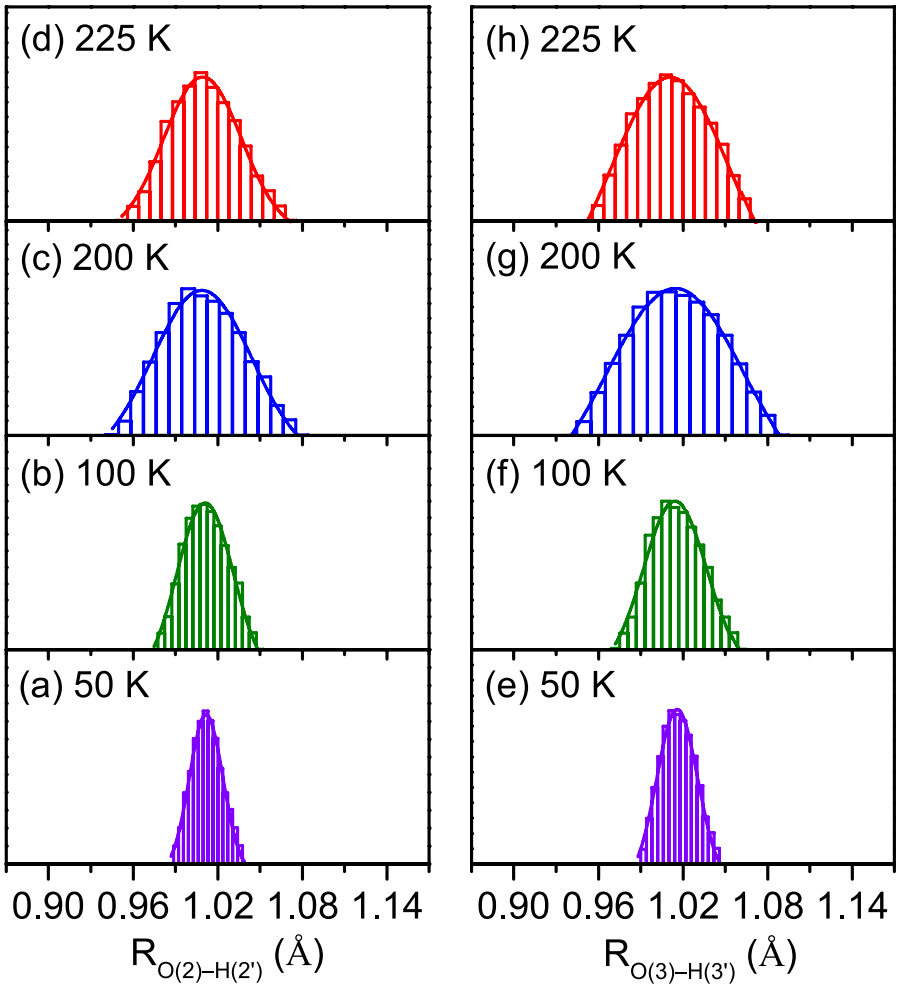

Figure S6. Normal distribution of O(2)–H(2′) and O(3)–H(3′) bond distances ($R_{O(2)–H(2')}$ and $R_{O(3)–H(3')}$) during AIMD simulations of isomer 2-i for $HGaOH(H_2O)_2$ at 50 K, 100 K, 200 K, and 225 K. The atom labelling is indicated in Figure 2.

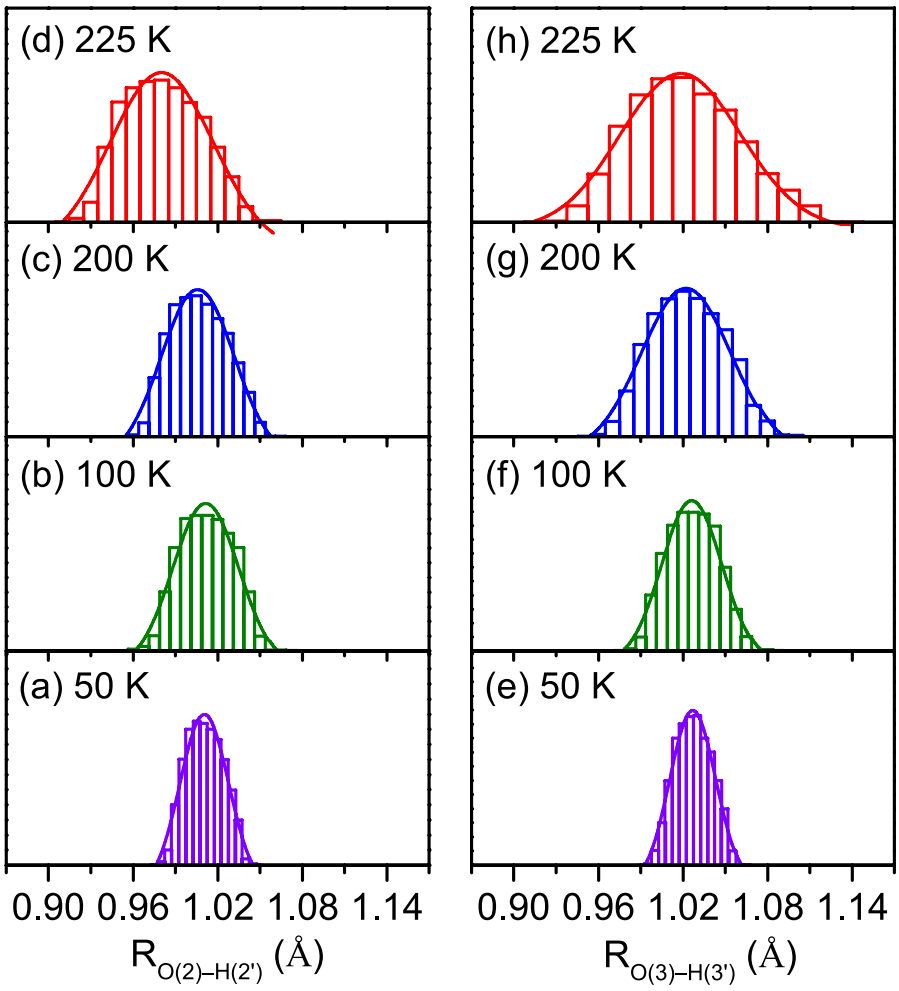

Figure S7. Normal distribution of O(2)–H(2′) and O(3)–H(3′) bond distances ($R_{O(2)–H(2')}$ and $R_{O(3)–H(3')}$) during AIMD simulations of isomer 2-I for $HAlOH(H_2O)_2$ at 50 K, 100 K, 200 K, and 225 K. The atom labelling is indicated in Figure 2.

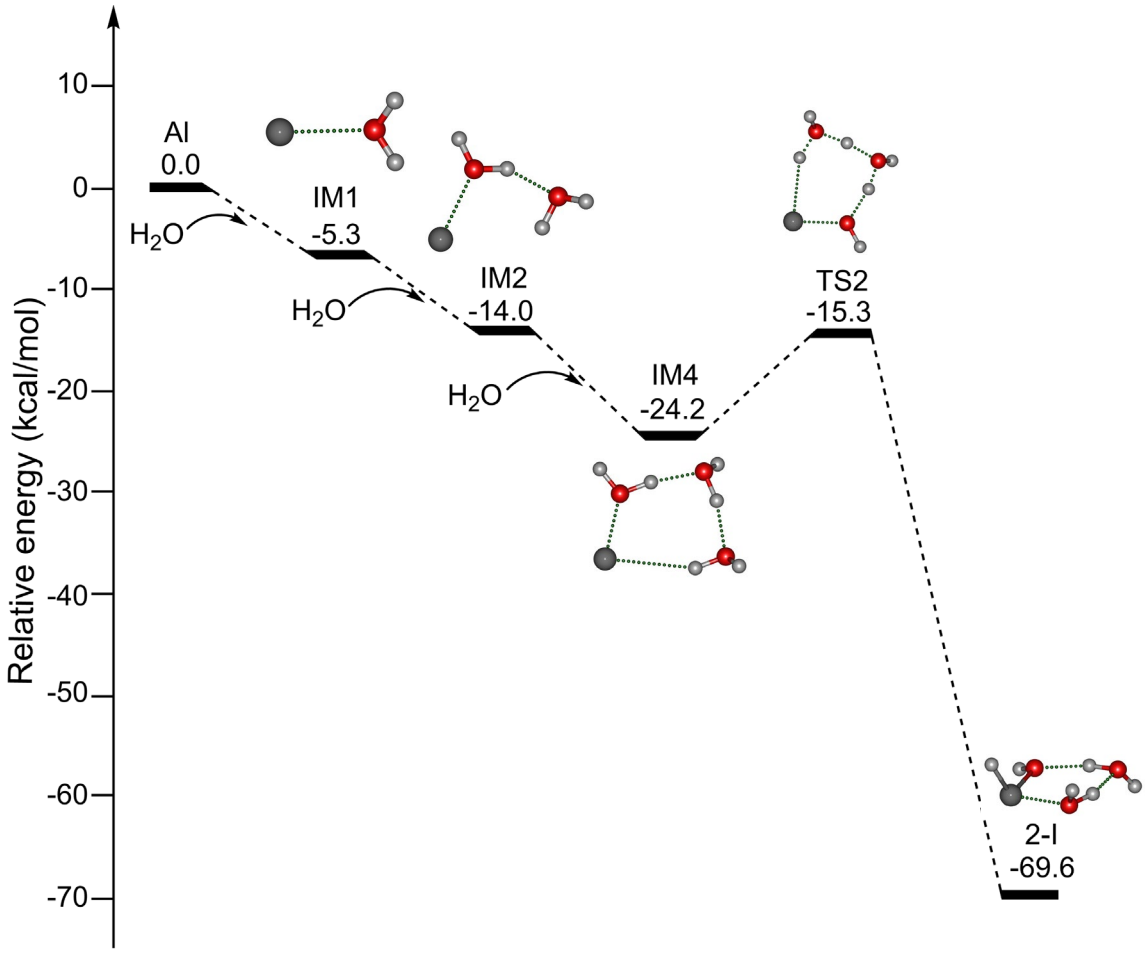

Figure S8. Potential energy profiles of pathway B for the formation of $HAlOH(H_2O)_2$ (isomer 2-I) calculated at the MP2/aug-cc-pVDZ level of theory. The abbreviation "IM" stands for intermediate and "TS" for transition state. The corresponding structures are embedded in the inset (O, red; H, light gray; Al, gray).

Table S1. Reaction energies of the formation of $HAlOH(H_2O)_2$ calculated at the MP2/aug-cc-pVDZ level of theory. Negative value of reaction energy denotes exothermicity.

Pathway	Reactions	Energy (kcal/mol)
A	$Al + H_2O \rightarrow Al(H_2O)$	-5.3
	$Al(H_2O) + H_2O \rightarrow Al(H_2O)_2$	-8.7
	$Al(H_2O)_2 \rightarrow HAlOH(H_2O)$	-41.7
	$HAlOH(H_2O) + H_2O \rightarrow HAlOH(H_2O)_2$	-13.9
B	$Al + H_2O \rightarrow Al(H_2O)$	-5.3
	$Al(H_2O) + H_2O \rightarrow Al(H_2O)_2$	-8.7
	$Al(H_2O)_2 + H_2O \rightarrow Al(H_2O)_3$	-10.2
	$Al(H_2O)_3 \rightarrow HAlOH(H_2O)_2$	-45.4

Cartesian coordinates of isomer 2-I, isomer 2-i, intermediates and transition states calculated at the MP2/aug-cc-pVDZ level of theory.

$HAlOH(H_2O)_2$ (isomer 2-I)

Al	1.41111000	-0.01822300	-0.11755400
O	-2.13425300	-0.07002500	0.12568800
H	-1.44289400	-0.78587200	0.09793000
O	0.17013500	-1.33874500	0.07664400
H	0.38679300	-2.21352700	-0.26536900
O	-0.01623000	1.40968200	-0.13440200
H	-0.93426400	0.99753400	-0.07408100
H	-2.73427700	-0.24999900	-0.60934000
H	2.15775000	0.45524100	1.22798400
H	0.06524200	2.02622500	0.60764600

$HAlOH(H_2O)_2$ (isomer 2-II)

Al	-2.28913000	-0.12553800	0.01666000
O	1.90865800	1.37370400	0.11005600
H	0.94302100	1.22472200	0.03475400
O	-0.55045100	0.07425100	-0.03408200
H	0.06547100	-0.68579200	-0.03264400
O	1.80909900	-1.41683900	-0.10094800
H	2.15445600	-0.50356300	-0.02604800
H	2.12175000	1.99412000	-0.59784500
H	-3.09663400	1.25579800	-0.01308000
H	2.23217800	-1.90222900	0.61808100

$HAlOH(H_2O)_2$ (isomer 2-III)

Al	-1.89884700	0.68214700	-0.00568100
H	1.92844700	2.10281000	-0.62243900
O	-0.94107400	-1.21875800	0.05378200
H	-1.36247900	-2.02330400	-0.27685700
O	1.66977800	1.49712200	0.08622400
H	0.68983300	1.60184000	0.14476000
O	1.68876500	-1.20834000	-0.10523900
H	1.83178800	-0.23024500	-0.07448500
H	0.05353600	-1.32068700	-0.00808500
H	2.20414200	-1.55852300	0.63282100

$HGaOH(H_2O)_2$ (isomer 2-i)

O	-2.54044800	-0.11318200	0.17696500
H	-1.82900900	-0.80838200	0.10603400
O	-0.24499300	-1.40512000	0.02761800
H	-0.08066900	-2.06775900	-0.65678200
O	-0.50207600	1.48407900	-0.21373700
H	-1.39022800	1.02767700	-0.12097600
H	-3.21162000	-0.34593800	-0.47651300
H	1.54031600	0.44087300	1.41188500
H	-0.46306700	2.13573500	0.50125900
Ga	1.02369100	-0.00349800	-0.02231200

H_2O

O	0.00000000	0.00000000	0.11908400
H	0.00000000	0.76051600	-0.47633500
H	0.00000000	-0.76051600	-0.47633500

IM1

Al	-0.02794700	-1.07609900	0.00000000
O	-0.02794700	1.30247600	0.00000000
H	0.29344700	1.78474100	-0.77542100
H	0.29344700	1.78474100	0.77542100

IM2

Al	0.30144000	0.79153600	-0.14122500
O	1.07938200	-0.80599800	0.14508200
H	1.89003900	-1.05755200	-0.30901900
H	-0.03167000	1.66232100	1.17018600
O	-1.43340300	-0.37671400	-0.11273700
H	-0.93927100	-1.20459000	0.06097800
H	-2.00565200	-0.22845200	0.65502600

IM3

Al	-1.53285600	-0.53830600	-0.00294800
O	2.03572300	-0.41881100	-0.10446100
H	1.35921000	-1.12241400	-0.02016100
O	-0.11797200	1.15341500	0.08509000
H	0.81302300	0.83902400	-0.01878400
H	2.64002000	-0.57730400	0.63415500
H	-0.22712400	1.98184400	-0.40192400

IM4

Al	-1.89884700	0.68214700	-0.00568100
H	1.92844700	2.10281000	-0.62243900
O	-0.94107400	-1.21875800	0.05378200
H	-1.36247900	-2.02330400	-0.27685700
O	1.66977800	1.49712200	0.08622400
H	0.68983300	1.60184000	0.14476000
O	1.68876500	-1.20834000	-0.10523900
H	1.83178800	-0.23024500	-0.07448500
H	0.05353600	-1.32068700	-0.00808500
H	2.20414200	-1.55852300	0.63282100

TS1

Al	-1.26401400	-0.51288000	0.00522100
O	1.76572700	-0.34203800	-0.10623700
H	2.21247300	-0.42540300	0.75652400
O	-0.17315400	1.05194600	0.02710300
H	1.08655000	0.51305500	-0.04793100
H	0.83113600	-1.07136000	-0.04771100
H	-0.43856400	1.97188100	-0.09568200

TS2

Al	1.69741500	-0.63191200	-0.03781500
H	-0.44313000	-1.43081000	-0.10956800
O	0.92113100	1.09522900	0.05403600
H	1.48390200	1.87229100	0.17408300
O	-1.52864900	-1.32474000	-0.06492200
H	-1.78265300	-1.72499400	0.78705400
O	-1.55419100	1.09540800	0.05365200
H	-1.63592500	-0.16796000	-0.00308300
H	-0.50214300	1.23319100	0.05569600
H	-1.89277000	1.50595900	-0.75470200

Supporting References

1 G. Li, C. Wang, Q. Li, H. Zheng, T. Wang, Y. Yu, M. Su, D. Yang, L. Shi, J. Yang, Z. He, H. Xie, H. Fan, W. Zhang, D. Dai, G. Wu, X. Yang and L. Jiang, *Rev. Sci. Instrum.*, 2020, **91**, 034103.

2 B. B. Zhang, Y. Yu, Z. J. Zhang, Y. Y. Zhang, S. K. Jiang, Q. M. Li, S. Yang, H. S. Hu, W. Q. Zhang, D. X. Dai, G. R. Wu, J. Li, D. H. Zhang, X. M. Yang and L. Jiang, *J. Phys. Chem. Lett.*, 2020, **11**, 851-855.

3 G. Li, C. Wang, H. J. Zheng, T. T. Wang, H. Xie, X. M. Yang and L. Jiang, *Chin. J. Chem. Phys.*, 2021, **34**, 51-60.

4 G. Li, H. Xie and L. Jiang, *J. Phys. Chem. Lett.*, 2024, **15**, 4806-4814.